

CONTROL OF A PERMANENT-MAGNET SYNCHRONOUS GENERATOR WIND TURBINE SYSTEM DURING GRID FAULT

Van Tan Luong*, Dang Ngoc Khoa

Ho Chi Minh City University of Food Industry

*Email: *luongvt@hufi.edu.vn*

Received: 26/9/2019; Accepted for publication: 6/12/2019

ABSTRACT

In this research, an enhanced control scheme for the permanent-magnet synchronous generator (PMSG) wind turbines under grid voltage fault condition is introduced. The machine-side converter (MSC) controls the DC-link voltage; however, this voltage value can be still increased during the grid fault. Thus, the braking chopper (BC) added to the DC-bus will be activated to dissipate the surplus power between the grid and generator powers. Meanwhile, the grid active power is regulated at the grid-side converter (GSC), from which can be exploited to inject reactive current into the grid for assisting the grid voltage recovery. Also, an algorithm of positive-sequence current control in the dq-axis is implemented, based on feedback linearization theory. The validity of this control algorithm has been verified by the simulation of the 2MW-PMSG wind turbine system.

Keywords: Braking chopper, permanent-magnet synchronous generator, unbalanced voltage, wind turbine.

1. INTRODUCTION

Recently, the wind power generation has been concerned as one of the most rapidly growing energy sources in the world since the natural resources are becoming exhausted. In the variable-speed wind turbine (WT) systems, a direct-drive wind energy conversion system based on permanent-magnet synchronous generator (PMSG) has a lot of advantages such as no gearbox, high precision, high power density, and simple control method, except initial installation costs [1 - 2].

In order to achieve objectives such as continuity and security, high levels of wind power are confronted with new challenges as well as other new approaches in the power system operation. Therefore, several nations have issued dedicated grid codes for connecting the wind power systems to the grid [3]. Lately, the micro- and smart-grid have been researched for the efficiency of power management [4]. However, the grid voltage in these systems is much fluctuated, compared with the conventional grid. Thus, robust control of the wind power generation system is required for grid variations.

Several different solutions have been proposed for low voltage ride-through (LVRT) technique or grid fault in the variable-speed wind turbine systems. For this, a braking chopper (BC) with advantage of the low cost and the simple control performance has been applied for the LVRT in the PMSG wind turbine systems [5 - 8]. However, it is so difficult to improve the power quality at the output of the wind turbine systems since the BC can just dissipate the surplus power between the grid and generator power. Also, a static synchronous compensator (STATCOM) installed at the point of common coupling (PCC) has been applied to keep the wind turbine system connected to the grid during grid faults [9 - 10]. With this method, the

voltage regulation is considerably improved in both transient state and steady-state. However, STATCOM can not be used alone without BC. In one way, an energy storage system (ESS) has been employed to give a ride-through capability and mitigate the output power fluctuations of the wind turbine systems [11 - 12]. In this method, to reduce the power capacity of the ESS which can absorb the full differential power during the grid fault, the generator speed can be increased to store the kinetic energy in the system inertia. Another method using a hybrid system of the ESS and the BC has been presented [13- 14], where the ESS consisting of electric double-layer capacitors (EDLC) and the BC are connected to the DC-link side of the back-to-back converters in the variable-speed wind turbine system. By switching the control mode, the ESS is operated to control the DC-link voltage to follow its reference value during the grid voltage sags, while the grid-side converter (GSC) is considered as a STATCOM to supply the reactive current to the grid for satisfying the reactive current requirements of the grid code. Thus, the grid voltage can be recovered rapidly without an external STATCOM after fault clearance. The generator active power can be absorbed fully by the ESS and the BC during the voltage sags. In addition, the output power fluctuation of wind turbine systems operating in steady state is smoothed by the ESS. With this control scheme, the system can still work well despite the full interruption of the grid voltage. However, the cost of the ESS system designed in the case of the voltage dip is too expensive.

In the PMSG wind turbine system, the generator is connected to the grid through the full-scale back-to-back converters. Conventionally, DC-link voltage is controlled to be a constant at the GSC, whereas the MSC controls the active power for maximum power point tracking (MPPT). In the case of the grid voltage sags, the GSC in the conventional control method may be out of control. For this reason, the DC-link voltage is excessively increased due to the continuous operation of WT and generator. The overall generated output power delivering to the grid can be restricted. To solve these problems, the DC-link voltage must be controlled by the MSC, whereas the GSC controls the MPPT [15]. With this method, the power mismatched between the turbine and the grid are stored in the inertia by increasing the generator speed. However, the amount of energy stored in the turbine inertia is not so large, when the generator works near the rated speed before the grid sags occur. Despite this, the response of the DC-link voltage still overshoot during the grid fault.

In the paper, the DC-link voltage is regarded to control at the MSC with the support of braking chopper. Meanwhile, the grid active power is regulated at the GSC, from which can be exploited to inject reactive current into the grid to recover fast grid voltage. The simulation results for the 2 MW-PMSG wind turbine system are provided to verify the effectiveness of the proposed method.

2. SYSTEM MODELING

Figure 1 shows configuration of the PMSG wind turbine system, which is connected the grid through full T-type three-level back-to-back pulse-width modulation (PWM) converters, where e_{ga} , e_{gb} , and e_{gc} represent the source phase voltages, and L and C denote the line inductance and the DC-link capacitances, respectively. Compared with the conventional three-level neutral-point clamped (NPC) converter, the count of diodes in the T-type converter is decreased by two per bridge leg [16 - 19]. The advantages of the T-type converter are that total harmonic distortion is low and the operating principle is simple. The modulation strategy for the three-level NPC converter is similar to the T-type converter.

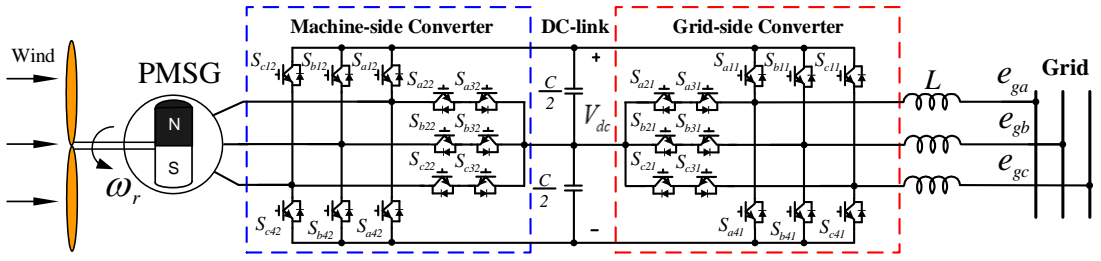


Figure 1. Circuit configuration of PMSG wind turbine system equipped with T-type back-to-back PWM converters.

3. CONTROL OF GRID-SIDE CONVERTER

3.1. Mathematical modelling

Under unbalanced voltage conditions, the grid voltages in positive and negative sequence components at the synchronous d-q frame are represented by [13 - 14]

$$E_d^+ = RI_d^+ + L \frac{dI_d^+}{dt} - \omega LI_q^+ + V_d^+ \quad (1)$$

$$E_q^+ = RI_q^+ + L \frac{dI_q^+}{dt} + \omega LI_d^+ + V_q^+ \quad (2)$$

$$E_d^- = RI_d^- + L \frac{dI_d^-}{dt} - \omega LI_q^- + V_d^- \quad (3)$$

$$E_q^- = RI_q^- + L \frac{dI_q^-}{dt} + \omega LI_d^- + V_q^- \quad (4)$$

where R and L are the input resistance and boost inductance of the grid-side converter, respectively. It is noted that the superscripts “+” and “-” are the positive- and negative-sequence components, respectively.

3.2. Current references

The reference of the positive-sequence current component in q-axis (I_q^{+*}) is achieved from the real power reference (P_0^*) determined from the MPPT method [15]

$$I_q^{+*} = \frac{2}{3} \frac{E_q^+}{D} P_0^* \quad (5)$$

$$\text{where } D = E_q^{+2} + E_d^{+2} - E_q^{-2} - E_d^{-2} \neq 0.$$

The positive-sequence component of the d-axis current reference or the grid reactive current, which is selected to support the grid voltage recovery, must satisfy the following condition as:

$$-\sqrt{I_{rated}^2 - I_q^{+*2}} \leq I_d^{+*} \leq \sqrt{I_{rated}^2 - I_q^{+*2}} \quad (6)$$

The dq-axis current references of negative-sequence components (I_{dq}^{-*}) are set to zero to eliminate the unbalanced current components flowing into the grid, which are expressed as

$$\begin{cases} I_d^* = 0 \\ I_q^* = 0 \end{cases} \quad (7)$$

3.3. Grid current controllers

The nonlinear state-space model of the grid-side converter is represented as

$$\begin{bmatrix} \dot{I}_d^+ \\ \dot{I}_q^+ \end{bmatrix} = \begin{bmatrix} -\frac{E_d^+}{L} - \frac{R}{L}I_d^+ + \omega I_q^+ \\ -\frac{E_d^+}{L} - \frac{R}{L}I_d^+ - \omega I_q^+ \end{bmatrix} + \begin{bmatrix} -\frac{1}{L} & 0 \\ 0 & -\frac{1}{L} \end{bmatrix} \begin{bmatrix} V_d^+ & V_q^+ \end{bmatrix} \quad (8)$$

$$\begin{bmatrix} \dot{I}_d^- \\ \dot{I}_q^- \end{bmatrix} = \begin{bmatrix} -\frac{E_d^-}{L} - \frac{R}{L}I_d^- + \omega I_q^- \\ -\frac{E_d^-}{L} - \frac{R}{L}I_d^- - \omega I_q^- \end{bmatrix} + \begin{bmatrix} -\frac{1}{L} & 0 \\ 0 & -\frac{1}{L} \end{bmatrix} \begin{bmatrix} V_d^- & V_q^- \end{bmatrix} \quad (9)$$

For the linearization, a relation between input and output should be delivered. Thus, the output y in (8) is differentiated as [20 - 21]

$$\dot{y} = \nabla h(f + g \cdot u) = L_f h(x) + L_g h(x) \cdot u \quad (10)$$

where $L_f h(x)$ and $L_g h(x)$ represent Lie derivatives of $h(x)$ with respect to $f(x)$ and $g(x)$, respectively. The Lie derivative is defined as [20 - 21]

$$L_f h = \nabla h f = \frac{\partial h}{\partial x} \cdot f \quad (11)$$

If $L_f h$ and $L_g h$ are replaced to $A(x)$ and $E(x)$, the output of the system is obtained as

$$\dot{y} = A(x) + E(x)u \quad (12)$$

where

$$A(x) = \begin{bmatrix} -\frac{E_d^+}{L} - \frac{R}{L}I_d^+ + \omega I_q^+ \\ -\frac{E_d^+}{L} - \frac{R}{L}I_d^+ - \omega I_q^+ \end{bmatrix} \text{ and } E(x) = \begin{bmatrix} -\frac{1}{L} & 0 \\ 0 & -\frac{1}{L} \end{bmatrix}$$

If a control input u is chosen as

$$u = E^{-1}(x)[-A(x) + v] \quad (13)$$

where v is the equivalent control input to be specified. The resultant dynamics become linear as

$$\dot{y} = \begin{bmatrix} v_1 \\ v_2 \end{bmatrix} = \begin{bmatrix} \dot{I}_d^+ \\ \dot{I}_q^+ \end{bmatrix} \quad (14)$$

To eliminate the tracking error in the presence of parameter variations, the new control inputs with an integral control is given by

$$\begin{cases} v_1 = \dot{y}_1^* - k_{11}e_1 - k_{12} \int e_1 dt \\ v_2 = \dot{y}_2^* - k_{21}e_2 - k_{22} \int e_2 dt \end{cases} \quad (15)$$

where $e_1 = y_1 - y_1^*$, $e_2 = y_2 - y_2^*$, y_1^* and y_2^* are the tracking references, and k_{11} , k_{12} , k_{21} and k_{22} are the controller gains.

If the all gains are positive, the tracking error converges to zero. From (15), we obtain error dynamics as

$$\begin{cases} \ddot{e}_1 + k_{12}\dot{e}_1 + k_{11}e_1 = 0 \\ \ddot{e}_2 + k_{21}\dot{e}_2 + k_{22}e_2 = 0 \end{cases} \quad (16)$$

By locating the desired poles on the left-half plane, the controller gains are determined and asymptotic tracking control to the reference is achieved [20]. The current controllers for positive-sequence components using FL, while the negative-sequence components using PI controller are shown in Figure 2.

4. CONTROL OF MACHINE-SIDE CONVERTER

The operation of the GSC is directly influenced by grid voltage sags, where the power delivered to the grid is restricted. During the grid fault duration, the wind turbine and generator keep operating, likes in normal condition. Thus, the power delivered from the machine side may increase the DC-link voltage excessively high. Unlike the conventional control of the AC/DC converter, the DC-link voltage is controlled by the MSC. The control structure of the MSC consisting of the outer DC-link voltage control loop and the inner current control loop are illustrated in Figure 2. In order to obtain maximum torque at a minimum current, the d-axis reference current component is set to zero and then the q-axis current is determined by the DC-link voltage controller.

5. BRAKING CHOPPER CONTROL

The braking chopper will be activated to dissipate the rest of the power, P_{bc} as

$$P_{bc} = P_g - P_{grid} \quad (17)$$

where P_g and P_{grid} are the generated and grid power, respectively.

As shown in Figure 2, the braking chopper is controlled by the switch S_3 . The duty ratio D_3 for the switch depends on P_{bc} , which is expressed as

$$D_3 = \frac{R_{bc}}{V_{dc}^2} P_{bc} \quad (18)$$

where R_{bc} is the braking resistance.

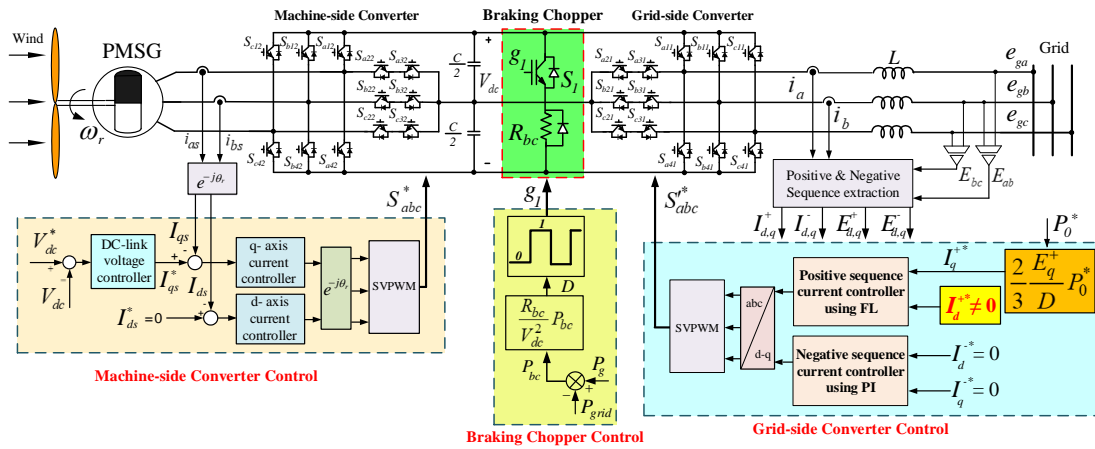


Figure 2. Proposed control block diagram of overall system.

6. SIMULATION RESULTS

To verify the effectiveness of the proposed method, the simulation using the PSIM software has been carried out for a 2-MW PMSG wind turbine. The parameters of the wind turbine and generator are listed in Table 1 and 2, respectively. The DC-link voltage is controlled at 1.3[kV], the DC-link capacitance is 0.1[F], the switching frequency is 2[kHz], and the grid voltage is 690[V_{rms}]/60[Hz].

Table 1. Parameters of wind turbine

Parameter	Value
Rated power	2 [MW]
Blade radius	45 [m]
Air density	1.225[kg/m ³]
Max. power conv. coefficient	0.411
Cut-in speed	3[m/s]
Cut-out speed	25[m/s]
Rated wind speed	16.1 [m/s]
Blade inertia	6.3×10 ⁶ [kg.m ²]

Table 2. Parameters of 2 MW- PMSG

Parameter	Value
Rated power	2 [MW]
Grid voltage	690 [V]
Stator voltage/frequency	690[V]/60[Hz]
Stator resistance	0.008556[Ω]
d-axis inductance	0.00359[H]
q-axis inductance	0.00359[H]

Figure 3 shows the system performance under the normal grid condition. The wind speed changes from 6 m/s to 8 m/s at 20 s and returns to 6 m/s at 50 m/s, as shown in Figure 3(a). For the pattern of the step-wise varying wind speed, the generator speed, turbine and generator powers vary, as illustrated from Figure 3(b) to 3(d), respectively, where the turbine power is proportional to the cube of the wind speed. Also, the turbine and generator torques are shown in Figure 3(e) and (f), respectively, which are proportional to the square of the wind speed. Figure 3(g) shows the power conversion coefficient according to the turbine speed, from which the wind turbine system is seen to track the maximum power point. In this case, the generator is controlled to keep the DC-link voltage constant, of which variation is less than 1% as shown in Figure 3(h).

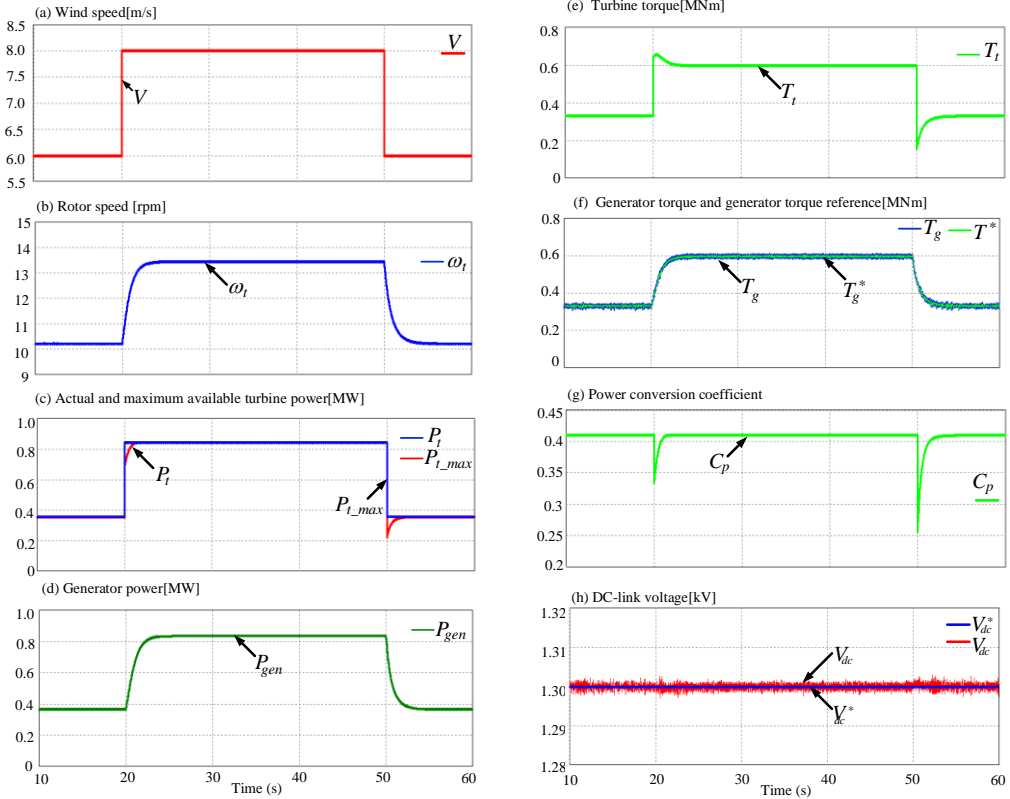


Figure 3. Responses of wind turbine system under normal grid voltage condition.

Figure 4 shows the system performance for grid unbalanced voltage sag, in which the wind speed is assumed to be constant (8 m/s) for easy examination. The fault condition is 20% sag in the grid A-phase voltage, 40% sag in the grid B-phase voltage, and 50% sag in the grid C-phase voltage, for 1 sec (60 cycles), which is between the point ① to ② as shown in Figure 4 (a). Due to the grid unbalanced voltage sag, the positive-sequence q-axis voltage is reduced and the negative-sequence dq-axis voltage components appear. The components of the grid positive- and- negative sequence currents in dq-axis are illustrated in Figure 4 (c) and (d), in which the reactive current component is injected to the grid, as shown in Figure 4 (d). It is noted that the reference value of the reactive current selected must satisfy the condition as given in (6). From controlling this reactive current at the GSC, the amount of the reactive power to support the grid voltage recovery under the grid fault is achieved in Figure 4 (e). Also, the grid, generator and turbine powers are also illustrated from Figure 4 (f) to 4 (g). During the grid fault duration, the generator speed in Figure 4 (h) is increased to keep the DC-link voltage constant thanks to the MPPT control method. Figure 4 (i) shows the response of

the DC-link voltage which is controlled by the MSC and the BC under unbalanced sags. Since the differential power is not able to deliver to the grid, the rest of the power is dissipated by the BC. The switching pulse for the BC control is shown in Figure 5 (j).

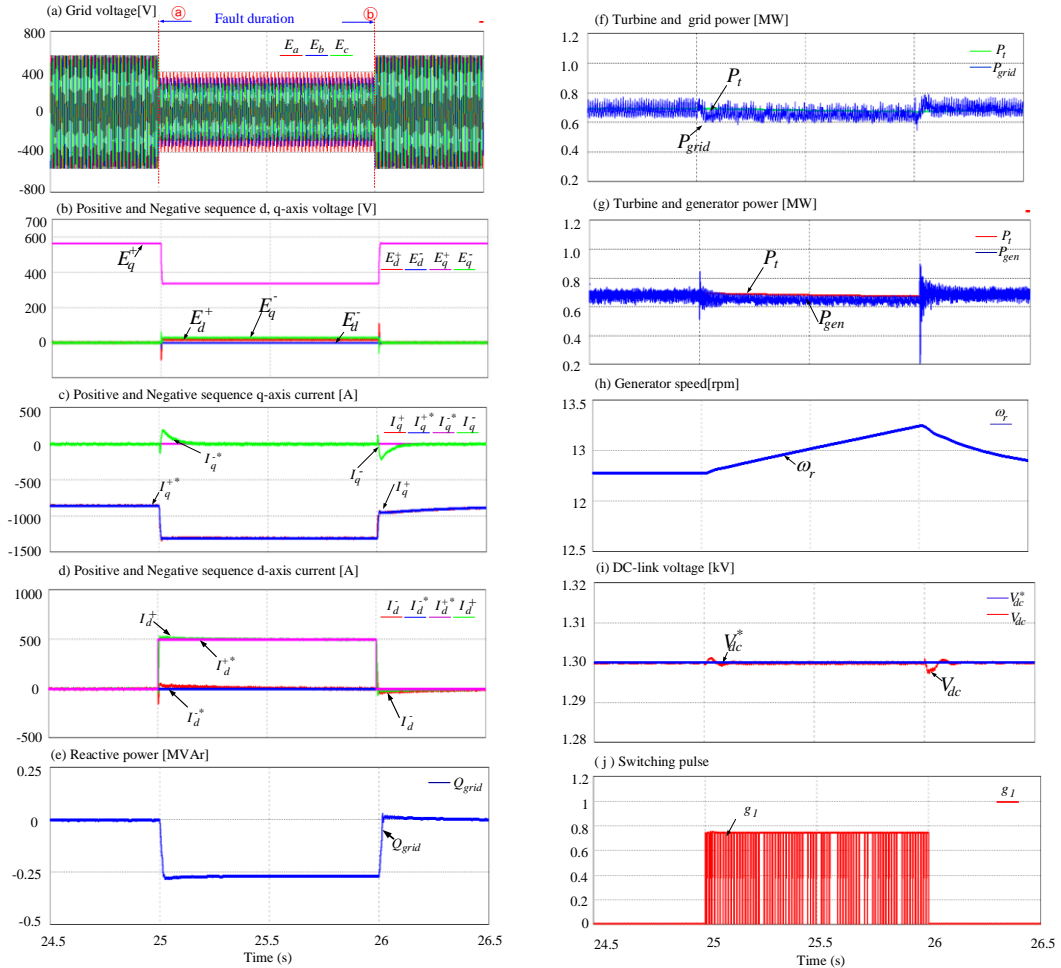


Figure 4. Performance of PMSG wind turbine system for unbalanced voltage sag.

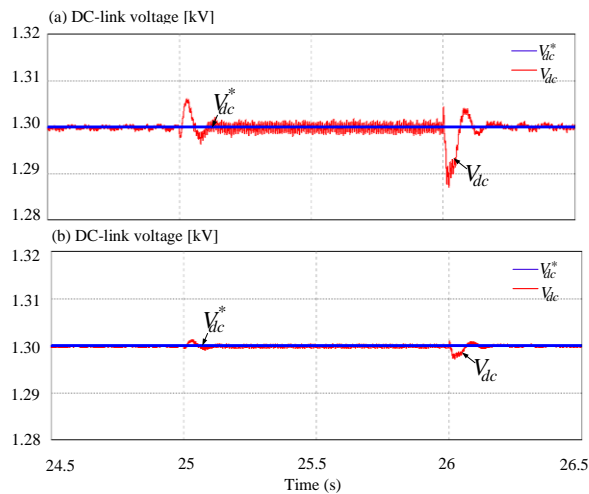


Figure 5. Performance of DC-link voltage control without (a) and with braking chopper (b).

Figure 5 shows the DC-link voltage responses without and with using BC. The percentage of the DC-link voltage error in case of using BC is so low (less than 1% in comparison to DC-link voltage reference), whereas this value without using BC is around 5%. By comparison, the proposed method gives faster transient response and lower overshoot.

7. CONCLUSION

The paper proposes a coordinated control scheme of grid-side converter, machine-side converter, and braking chopper in the permanent-magnet synchronous generator wind turbine system under grid fault condition. At the grid fault, the DC-link voltage is controlled at the machine-side converter, while the grid active power is controlled at the grid-side converter, from which can be exploited to inject reactive current into the grid for supporting the grid voltage recovery. Also, BC is proposed to dissipate the surplus power between the grid and generator powers. The validity of the control algorithm has been verified by simulation results for 2 MW-PMSG wind power system.

REFERENCES

1. Akhmatov V. - Analysis of dynamic behavior of electric power systems with large amount of wind power, Ph.D. dissertation, Department of Electrical Power Engineering, Technical University of Denmark, Kongens Lyngby, Denmark, April 2003.
2. Chinchilla M., Arnaltes S., Burgos J.C. - Control of permanent magnet generators applied to variable-speed wind-energy systems connected to the grid, *IEEE Transactions on Energy Conversion* **21** (1) (2006) 130-135.
3. Iov F., Hansen A.D., Sørensen P., Cutululis N. A. -Mapping of grid faults and grid codes, Technical Report Risø-R-1617(EN), Risø National Laboratory, Technical University of Denmark, Roskilde, Denmark (2007).
4. Robert Pollin, H Garrett-Peltier, and H Scharber - Green recovery: A new program to create good jobs and start building a low-carbon economy, Center for American Progress (2008).
5. Brando G., Coccia A., Rizzo R. - Control method of a braking chopper to reduce voltage unbalance in a 3-level chopper, *IEEE International Conference on Industrial Technology* **2** (2004) 975-978.
6. Conroy J. F., Watson R. - Low-voltage ride-through of a full converter wind turbine with permanent magnet generator, *IET Renewable Power Generation* **1** (3) (2007) 182-189.
7. Li W., Abbey C., Joos G. - Control and performance of wind turbine generators based on permanent-magnet synchronous machines feeding a diode rectifier, *37th IEEE Power Electronics Specialists Conference* (2006) 1-6.
8. Qais M. H., Hasanién H. M., Alghuwainem S. - Low voltage ride-through capability enhancement of grid-connected permanent-magnet synchronous generator driven directly by variable speed wind turbine: a review, *The Journal of Engineering* **2017** (13) (2017) 1750-1754.
9. Singh B., Saha R., Chandra A., Al-Haddad K. - Static synchronous compensators (STATCOM): a review, *IET Power Electronics* **2** (4) (2009) 297-324.
10. Wang L., Kerrouche K. D. E., Mezouar A., Bossche A. V. D., Draou A., Boumediene L. - Feasibility Study of wind farm grid-connected project in Algeria under grid fault conditions using D-FACTS devices, *Applied Sciences* **8** (11) (2018) 1-22.
11. Nguyen T. H., Lee D.-C. - Ride-through technique for PMSG wind turbines using energy storage systems, *Journal of Power Electronics*, **10** (6) (2010) 297-324.

12. Abedi M. R. and Lee K. Y. - Smart energy storage system for integration of PMSG-based wind power plant, 2015 IEEE Power & Energy Society General Meeting (2015) 1-5.
13. Nguyen T. H., Lee D.-C. - Advanced fault ride-through technique for PMSG wind turbine systems using line-side converter as STATCOM, IEEE Transactions on Industrial Electronics **60** (7) (2013) 2842-2850.
14. Tan Luong Van and Ho V. C. - Enhanced fault ride-through capability of DFIG wind turbine systems considering grid-side converter as STATCOM, Lecture Notes in Electrical Engineering **371** (2015) 185-196.
15. Van T. L., Nguyen T. D., Tran T. T., and Nguyen H. D., -Advanced control strategy of back-to-back PWM converter in PMSG wind turbine system, Advances in Electrical and Electronic Engineering (AEEE)-Power Engineering and Electrical Engineering, **13** (2) (2015) 81–95.
16. Kolar J. W. - High efficiency drive system with 3-level T-type inverter, Proceedings of the 2011 14th European Conference on Power Electronics and Applications (2011) 1-10.
17. Schweizer M., Kolar J.W. - Design and implementation of a highly efficient three level T-type converter for low-voltage applications, IEEE Transactions on Power Electronics **28** (2) (2013) 899-907.
18. Shin S.-M., Ahn J.-H., Lee B.-K. - Maximum efficiency operation of three level T-type inverter for low-voltage and low-power home appliances, Journal of Electrical Engineering Technology **10** (2) (2015) 286-294.
19. Kim T.-H., Lee W.-C. - Level change method for higher efficiency of a 3 level T-type converter, 2018 21st International Conference on Electrical Machines and Systems (ICEMS) (2018) 741-744.
20. Van T. L., Nguyen N. M. D., Toi L. T., Trang T. T. - Advanced control strategy of dynamic voltage restorers for distribution system using sliding mode control input-output feedback linearization, Lecture notes in electrical engineering **465** (2017) 521-531.
21. Chen C. T. - Linear System Theory and Design, Press, New York: Oxford University, 1999.

TÓM TẮT

ĐIỀU KHIỂN HỆ THỐNG TUA-BIN GIÓ DỪNG MÁY PHÁT PMSG TRONG TRƯỜNG HỢP LƯỚI SỰ CỐ

Văn Tấn Lượng*, Đặng Ngọc Khoa
Trường Đại học Công nghiệp Thực phẩm TP.HCM
*Email: luongvt@hufi.edu.vn

Nghiên cứu này giới thiệu chiến lược điều khiển nâng cao cho tua-bin gió dừng máy phát đồng bộ nam châm vĩnh cửu (PMSG) trong điều kiện sự cố điện áp lưới. Bộ chuyển đổi công suất phía máy phát (MSC) điều khiển điện áp DC-link; tuy nhiên, giá trị điện áp này vẫn có thể tăng lên trong khoảng thời gian sự cố lưới điện. Vì thế, braking chopper (BC) được thêm vào thanh cái DC sẽ được kích hoạt để tiêu tán công suất dư giữa lưới điện và máy phát. Trong khi đó, công suất tác dụng lưới được điều khiển bởi bộ chuyển đổi công suất phía lưới (GSC), có thể được khai thác để bơm dòng điện phản kháng vào lưới, hỗ trợ cho việc phục hồi điện áp lưới. Ngoài ra, thuật toán điều khiển dòng thứ tự thuận trong hệ trục dq được triển khai, dựa vào lý thuyết tuyến tính hóa hồi tiếp. Tính hợp lý của thuật toán điều khiển này đã được kiểm chứng bằng việc mô phỏng hệ thống tua-bin gió dừng máy phát PMSG công suất 2MW.

Từ khóa: Braking chopper, máy phát đồng bộ nam châm vĩnh cửu, điện áp không cân bằng, tua-bin gió.